Thermo-Mechanical Stress in Electrical Contacts due to Arcing Events

Timo Mützel, Michael Bender, Frank Heringhaus
Umicore AG & Co. KG
Hanau-Wolfgang, Germany
timo.muetzel@eu.umicore.com

Duancheng Ma
Max-Planck-Institut für Eisenforschung GmbH
Düsseldorf, Germany

***Abstract*—Silver tin oxide (Ag/SnO_2) contact materials are widely used for relays and contactor applications. A general trend in these applications is the steady miniaturization of switching devices, resulting in growing energy densities to be handled. The higher arcing energy densities in such new designs are inducing increased thermo-mechanical stresses in the contact material. As these stresses cannot be measured, FEM simulation was applied to make them visible for heavy duty break arcs. Based on these simulations and the understanding of the material stress behavior of the complete system (sub-assembly) significant improvements can be achieved.**

As contact materials are process driven products, a new generation of Ag/SnO_2 materials with adopted stress release behavior was developed. Basis for these developments were thermo-mechanical FEM simulations on material behavior during processing and application. A particular focus in this optimization was placed on the rolling and cladding processes as final production steps. The significant improvements by optimized Ag/SnO_2 contact materials were finally proven by heavy duty endurance tests in contactor applications and have been benchmarked against other production technologies, e.g. sintered Ag/SnO_2 contacts.

Keywords—contact material; silver tin oxide; thermo-mechanical stress

I. INTRODUCTION

Silver tin oxide (Ag/SnO_2) contact materials are widely used for relays and contactor applications. A general trend in these applications is the steady miniaturization of switching devices, resulting in growing energy densities to be handled. In addition, miniaturization and design to cost call for smaller contact tips, which are typically realized by a reduction in thickness, while the other dimensions are maintained. For contact material, these two aspects translate into the need for lower material erosion to fulfill endurance requirements, which is realized for Ag/SnO_2 by increased total metal oxide contents and the use of appropriate dopants [1].

Moreover, the higher arcing energy densities in such new designs are inducing increased thermo-mechanical stresses in the contact material. As these stresses cannot be measured, FEM simulation was applied to make them "visible" for heavy duty break arcs.

II. FEM ANALYSIS

Target of thermo-mechanical modelling was studying the impact of break arcs during contactor AC-4 heavy duty endurance testing. The geometry of the component and the layout of the materials are shown in Fig. 1. During each operation, the heat generated by the electric arc will induce thermal stress in the component. Hence, the heat transfer analysis and mechanical analysis were conducted by using finite element method (FEM) on the platform of Abaqus/Standard.

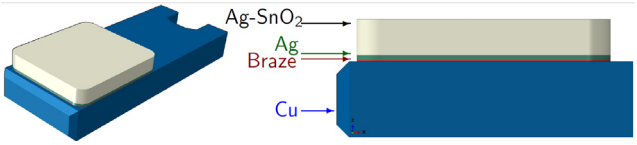

Fig. 1. Geometry and materials layout.

The movable contact of a 45 kW contactor switching under AC-4 conditions was modelled, and the arc root was modelled as a thermal power input. The mesh and the area of the thermal power input is shown in Fig. 2. Due to the symmetry of the movable contact, only half of the movable contact was modelled. The shape of the thermal power input area is approximated to be circular (red area in Fig. 2). The thermal power input area is placed near the edge of the contact material, so as to simulate the worst case scenario in which the contact materials are eroded faster and the component fails sooner in comparison with the case when this area is placed right in the middle of the contact materials. The diameter of this circular area, as well as the arc power and its duration, are listed in Table I. These parameters are derived from the experiments in Chapter IV as described in [2].

TABLE I. HEAT INPUT PARAMETERS FOR SIMULATION

Parameter	Value
arc spot diameter	1.25 mm
arc power	1 kW
arc duration	2.5 ms

As mentioned above, the heat transfer analysis and mechanical analysis were conducted. Thus, the necessary materials properties to carry out the simulation are the thermo-physical (the thermal conductivity, the expansion coefficients, and the heat capacity) and the mechanical properties (the elastic and plastic properties) of the materials shown in Fig. 1. The material properties input will be detailed in another publication.

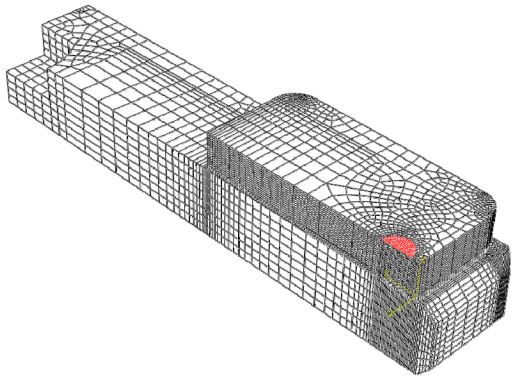

Fig. 2. Mesh and boundary condition. The area of the thermal power input is in red color

The resulting temperature distributions at 2.5 ms (when the thermal power input ends) is shown in Fig. 3. It shows that the highest temperature that the contact material endures could be close to the melting point of pure Ag, which is 1234.8 K. After arcing, at the thermal equilibrium, the temperature of the whole component increases by about 1 K.

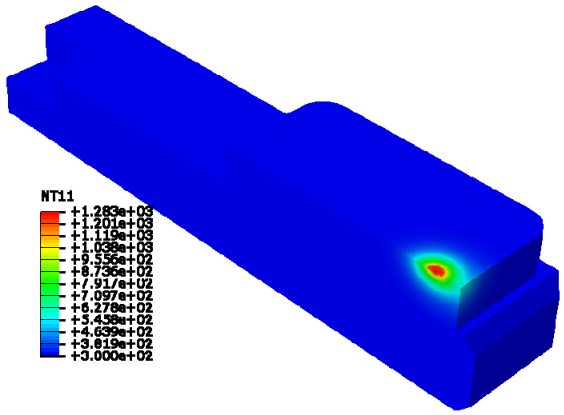

Fig. 3. Temperature distribution (in Kelvin) at 2.5 ms

The stress (σ_{33}) distribution after arcing, at the thermal equilibrium, is shown in Fig. 4. This stress component - σ_{33} - is the critical stress component to tear the Ag and the contact material layer apart, and also the magnitude of this stress component is found to be much higher than the other components. At 2.5 ms, the interface between the Ag and the contact material layer is found to be under tensile stress in the interior of the component, and it is under compression near the surface. The magnitude of the compressive stress is also high enough to undergo plastic deformation in silver. After arcing at thermal equilibrium, the stress state in the interior and at the free surface is exchanged, i.e. in the interior it is under compression, and the at the free surface it is under tension (see Fig. 4)

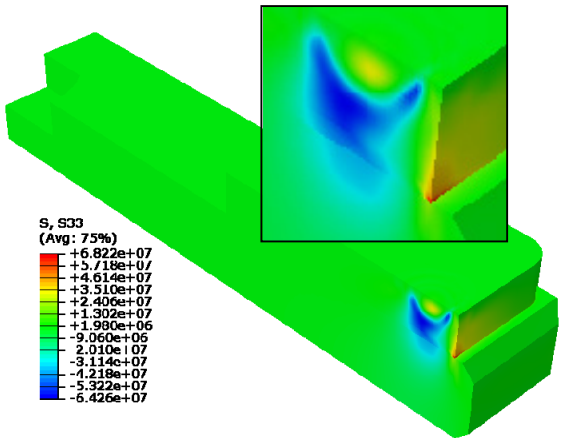

Fig. 4. Stress (σ_{33} in Pascal) distribution after arcing (1 cycle)

The stress evaluation between the free surfaces of Ag and Ag/SnO_2, simulating multiple switching cycles, is shown in Fig. 5. Here, the evolution of σ_{33} with switching cycle is illustrated in detail.

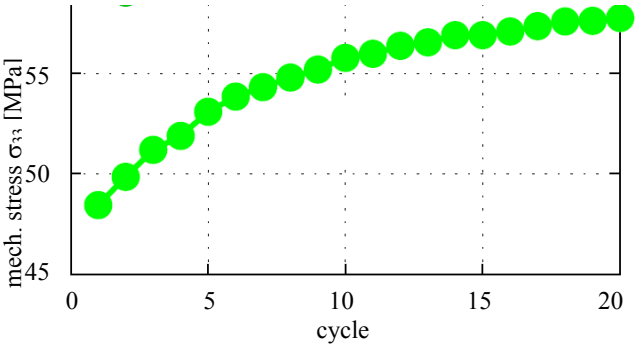

Fig. 5. Stress evaluation simulating multiple switching cycles (σ_{33}/MPa)

III. MATERIALS UNDER TEST

The contact material Ag/SnO_2 86/14 PMT3, with Bi_2O_3 and CuO dopants, was chosen as standard composition for all following tests.

Production of sintered contacts

According to the above composition starting powders of Ag (x90 = 41 µm), SnO_2 (x90 = 5.4 µm), Bi_2O_3 (x90 = 4 µm) and CuO (x90 = 1 µm) were intensely dry-blended in an Eirich mixer. In order to produce bi-metal contact tips, in a first step fine Ag powder and in a second one the powder mixture were filled into a die and pressed to greenings with a density of approximately 80% of the theoretical density. After sintering greenings at 900°C, for two hours under air atmosphere, sintered pieces were re-pressed in order to achieve final densities of around 97%.

Production of (co-)extruded contact materials

Same powder mixture as for sintered contacts was used for the extrusion process. Therefore powders were intensively mixed in an Eirich mixer. The powder blend was homogeneously filled into polymer tubes and densified in an isostatic press to green billets. After sintering at 800°C for 2 hours under air atmosphere, the billets were extruded to strips. Solid strips were hot cladded with Ag and braze (CuP 284) to final dimension.

For the co-extrusion process, green billets were mantled by silver sheets and extruded in indirect operation mode. Extruded bi-metal strips were cladded with braze alloy (CuP 284) and rolled to final dimension.

Production of extruded and hot-cladded contact materials following the plus approach

Based on simulation results, pre-material properties were adjusted in order to reduce stress at the bonding area. Therefore particle size distribution and heat treatment prior and following the cladding process were optimized with focus on reducing mismatch in deformation behavior of bonding partners in the gauge. Starting powders showed x90 values of 41 µm (Ag), 1.9 µm (SnO_2), 4 µm (Bi_2O_3) and 1 µm (CuO). After intense mixing powders were compacted to a billet and subsequently heat treated to obtain grain growth fine-tuning mechanical properties achieved after extrusion process. Bonding partners Ag (continuous casted & rolled), Braze (CuP 284) and extruded contact material strips were separately heated to specific working temperatures and hot cladded between 550°C and 750°C.

Assembling Process

All manufactured types of contact tips were induction brazed with identical parameter set-up for endurance testing, while the bonding area was checked by ultra-sonic inspection. As area of bond is one important factor impacting endurance results [3, 4].

IV. EXPERIMENTAL SET-UP

Endurance tests applying a 45 kW contactor were performed under ohmic load conditions with switching currents in the range of 4 times rated current to benchmark he different Ag/SnO_2 material samples. Table II summarizes the electrical test parameters.

TABLE II. TEST PARAMETERS 45 KW CONTACTOR

Parameter	Value
voltage U	400 V
current I	324 A
power factor $cos\varphi$	1
switching frequency	250 1/h
number of operations	120,000

The make and break operations were closely monitored during the endurance test. Therefore, phase currents and voltages across contacts $u_c(t)$ were measured. Arcing energies stressing the contact material were calculated based on these measurements. The average bounce arc energy at contact make W_{make} per phase was estimated by applying Eq. 1:

$$W_{make} = U_{AC} \int_{t_{bounce}} i(t)\, dt \tag{1}$$

where t_{bounce} represents the bouncing time (open contacts after initial contact make).

The calculation of the average arcing energy at contact break W_{break} per phase of a contactor providing a double breaking system was done in accordance to Eq. 2. Here, twice (double breaking) the anode cathode voltage drop U_{AC} is multiplied with the integral of the phase current from contact opening t_1 until an arcing voltage of 100V is reached, which equals the commutation time.

$$W_{break} = 2 \cdot U_{AC} \int_{t_1}^{t_{100V}} i(t)\, dt \tag{2}$$

The monitored average arcing energies – calculated in accordance to Eq. 1 and Eq. 2 – are summarized in Table III. Comparable values are a sign for mechanically stable and comparable devices, and therefore comparable boundary conditions for the electrical tests. Bounce arc energies at make operation W_{make} are in a range from 3 to 10 Ws, depending on synchronism, phase delay, and bounce behavior. Average break arc energies W_{break} can be observed in a range from 10 to 20 Ws.

TABLE III. AVERAGE ARCING ENERGIES

	Conventionally Cladded			*Sintered Contact*		
	L1	L2	L3	L1	L2	L3
avg. bounce arc energy W_{make} [Ws]	3.3	8.4	4.4	4.4	5.5	3.0
avg. break arc energy W_{break} [Ws]	12.5	16.1	16.1	12.5	9.7	15.5
	Co-Extruded			*Advanced Cladded*		
	L1	L2	L3	L1	L2	L3
avg. bounce arc energy W_{make} [Ws]	2.8	10.4	5.6	2.7	10.5	6.5
avg. break arc energy W_{break} [Ws]	12.9	13.7	17.9	19.3	10.4	15.9

V. RESULTS AND DISCUSSION

Material loss of the electrical contacts is dominated by vaporization and splash erosion of molten material under applied test conditions. The erosion behavior for all material variants is illustrated in Fig. 6. The total mass loss of contact material per electrical phase, which was measured by weighing the contact parts before and several times during testing, is plotted over the respective average arcing energy at break for this phase taken from Table III. This can be done as erosion is dominated by break arc under the applied test conditions – see arcing energy levels in Table III. All four materials show a comparable mass loss under these test conditions.

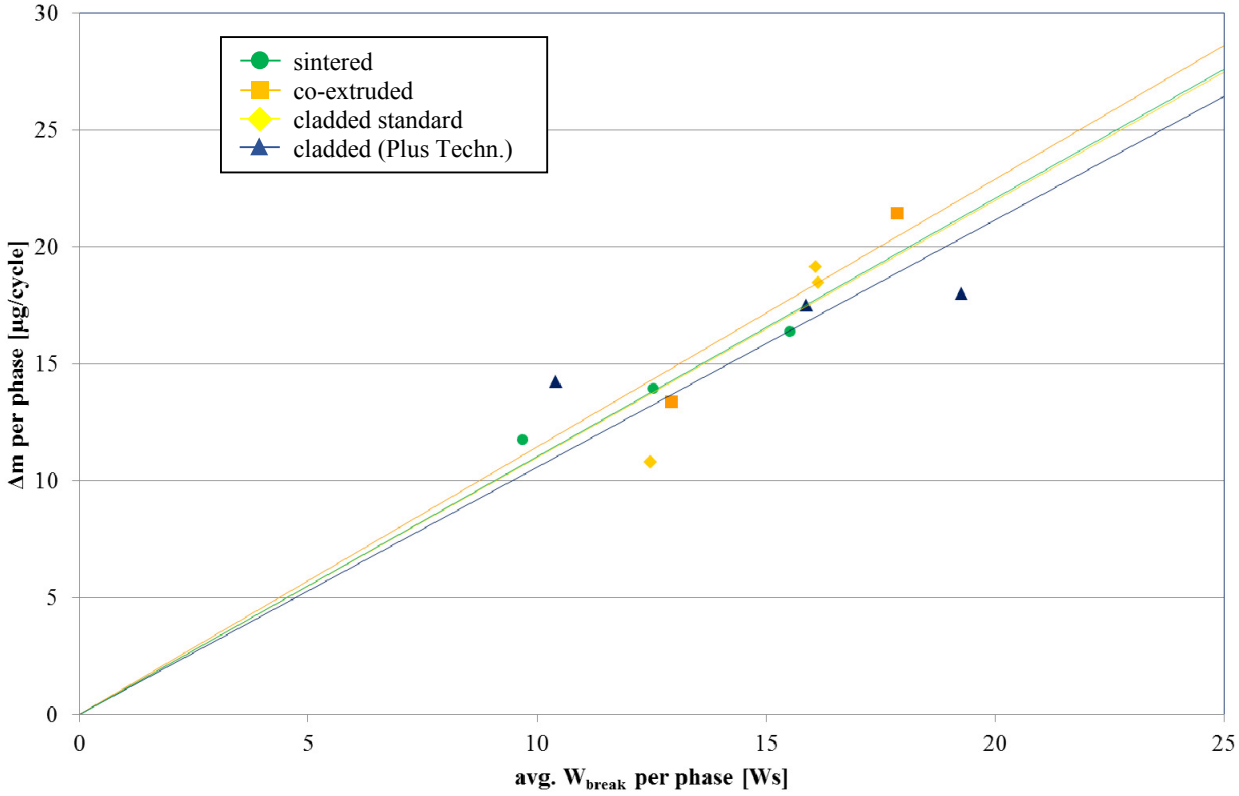

Fig. 6. Material loss over energy at break of different samples

After the endurance test, cross sections of all tested contact parts were performed to evaluate the changes in the microstructure caused by arcing. Fig. 7 is showing the standard Ag/SnO_2 86/14 PMT3 material manufactured by extrusion and classical hot cladding technology after endurance test.

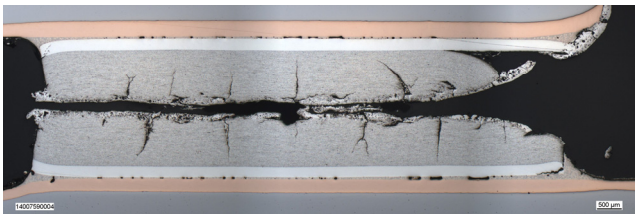

Fig. 7. Cross section of conventionally cladded material after test

The thermo-mechanical stresses are leading to formation of cracks in the Ag/SnO_2 material and a delamination of the contact material from the pure silver layer at the edge of the movable (upper) contact. On the stationary (lower) contact a crack in the brazing zone is already visible as well. The higher stressed right side of the contacts are in the direction of arc movement.

Fig. 8 is showing the co-extruded Ag/SnO_2 material after endurance test. Here as well the arcing formed similar vertical thermo-mechanical cracks in the contact material and in the cooperatively thick silver layer. In addition the material delaminates not in the bond between the silver and the contact material, but within the brazing alloy diffusion zone – as the zone with lowest withstand capability against the stresses.

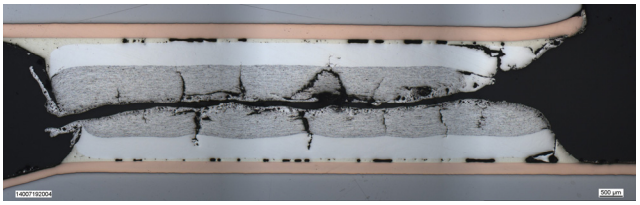

Fig. 8. Cross section of co-extruded material after test

The cross section of the sintered Ag/SnO_2 contact tip variant after test is illustrated in Fig. 9. Cracks along the granulate boundaries can be observed in addition to the vertical cracks.

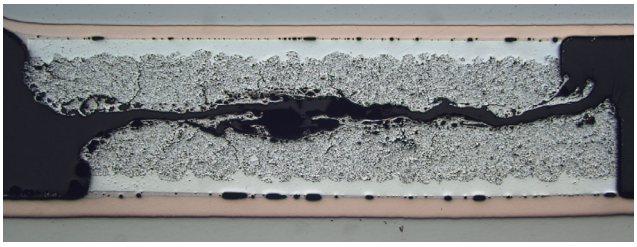

Fig. 9. Cross section of sintered material after test

Fig. 10 shows the cross section of the new Ag/SnO_2 86/14 PMT3 Plus material, manufactured by extrusion and advanced hot cladding technology. No more horizontal cracks appear in the contact tip, due to the much higher bonding strength between silver and contact material, which was achieved by fitting the two materials together based on the simulation results in Chapter 2. But, similar to the co-extruded material a next week boundary from silver into brazing joint can already be foreseen by the delamination in that zone, and will therefore be part of future studies.

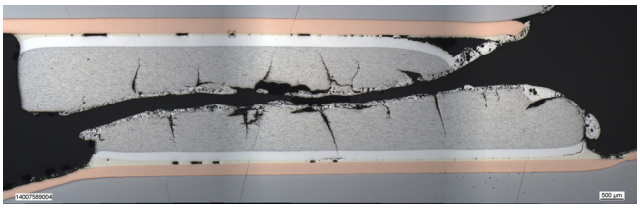

Fig. 10. Cross section of advanced material after test

VI. CONCLUSIONS

Higher arcing energy densities in new switching device designs are inducing increased thermo-mechanical stresses in the contact material. As these stresses cannot be measured, FEM simulation was applied to make them visible for heavy duty break arcs.

As contact materials are process driven products, a new generation of Ag/SnO_2 materials with adopted stress release behavior was developed. Basis for these developments were thermo-mechanical FEM simulations on material behavior during processing and in application. A particular focus in this optimization was placed on the rolling and cladding processes as final production steps. The significant improvements seen in the optimized Ag/SnO_2 contact materials were finally proven by endurance tests in contactor applications and have been benchmarked against other production technologies e.g. sintered Ag/SnO_2 contacts.

The advantages of Ag/SnO_2 materials produced by enhanced processing technology via extrusion and rolling are – in addition to performance improvements – the lower total thicknesses that can be realized as compared to sintered contacts, improved layer stability, and the possibility to produce strips for automated brazing processes. All three of these improvements are key for fulfilling the requirements of ongoing contact material volume reduction.

More than 100 electrical tests in different contactor ratings from 20 – 250 kW including full load AC-4 and AC-3 endurance test prove stability of the advanced cladding method. Studies on non-precious metal sub-layer cladding, and improvements in the mechanical strength of the brazing joints will be part of future work.

ACKNOWLEDGEMENT

The German Federal Ministry of Education and Research (PTJ/BMBF, #03X3586A) supported part of this research.

REFERENCES

[1] Mützel, T.; Niederreuther, R.: Contact Material Combinations for High Performance Switching Devices, 58th IEEE Holm Conference on Electrical Contacts, Portland, OR, USA, 2012

[2] Lindmayer, M.: Modeling of contact heating and erosion under arc influence, 24th International Conference on Electrical Contacts, St. Malo, France, 2008

[3] Wintz, J.-L.; Hardy, S.; Bourda, C.: Influence on the electrical performances of assembly, 24th International Conference on Electrical Contacts, St. Malo, France, 2008

[4] Späth, D; Behrens, V.; Finkbeiner, M.; Lutz, O.: Einfluss des Bindeanteils von Kontaktauflagen auf den Kontaktabbrand, 18. Albert-Keil-Kontaktseminar, Karlsruhe, Germany, 2005